

Deep BOO: Automating Beam Orientation Optimization in Intensity-Modulated Radiation Therapy

Olalekan Ogunmolu*, Michael Folkerts*, Dan Nguyen*, Nicholas Gans[†], and Steve Jiang*

*Department of Radiation Oncology, UT Southwestern Medical Center,
2280 Inwood Road, Dallas, Texas 75390-9303, USA

[†]Department of Electrical Engineering, University of Texas at Dallas,
Richardson, TX 75080, USA

{olalekan.ogunmolu, dan.nguyen, steve.jiang}@utsouthwestern.edu,
michael.folkerts@varian.com, ngans@utdallas.edu

Abstract. Intensity-Modulated Radiation Therapy (IMRT) is a method for treating cancers by aiming radiation to cancer tumor(s) while minimizing radiation to organs-at-risk from a robot’s tool frame. Computationally finding the correct treatment plan for a target volume is often an exhaustive combinatorial search problem where traditional optimization methods have not yielded real-time feasible results. Aiming to automate the beam orientation and intensity modulation process, we introduce a novel set of techniques leveraging (i) pattern recognition, (ii) monte carlo evaluations, (iii) game theory, and (iv) neuro-dynamic programming. We optimize a deep neural network policy that guides Monte Carlo simulations of promising beamlets. Seeking a saddle equilibrium, we let two fictitious neural network players, within a zero-sum markov game framework, alternately play a best response to their opponent’s mixed strategy profile during episodes of a two-player markov decision game. During inference, the optimized policy predicts feasible beam angles on test target volumes. This work merges the beam orientation and fluence map optimization subproblems in IMRT sequential treatment planning system into one pipeline. We formally introduce our approach, and present numerical results for coplanar beam angles on prostate cases.

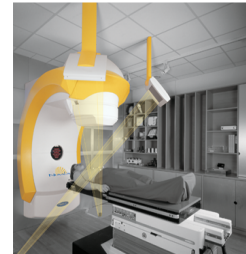
1 Introduction

In this paper, we will present the preliminary results of a multi-disciplinary research project whose goal is to design a real-time feasible treatment planning optimization in intensity-modulated radiation therapy (IMRT). IMRT is a cancer treatment method that delivers geometrically-shaped, high-precision x-rays or electron beams to tumors by modulating the intensity of the radiation beam from a robot’s eye-view. A multileaf collimator shapes a conventional geometrical field and the intensity of the geometric field shape is varied bixel-wise in order to modulate the “fluence” profile around a tumor. This is done while the patient lies in a supine position on a treatment table. Before treatment, a doctor contours the **critical structures** (or tumors) and **organs-at-risk** (or OARs) within a **target volume** (region of the patient’s computed tomography (CT) or magnetic resonance (MRI) scan that contains the tumor and other organs) and then

prescribes doses that must be delivered. Each beam to be delivered consists of beamlets, aimed from the same angle, where each beamlet may be of a different intensity from that of its neighbors. Radiation intensities may be delivered from about 5 – 15 different beam orientations with multiple collimator units. The process of choosing what beam angle is best for delivering beamlet intensities is termed **beam orientation optimization** (BOO) while the process of determining what intensity meets a prescribed fluence profile by a doctor is termed **fluence map optimization** (FMO).

A good radiation profile “influence” (fluence) matrix is obtained by simultaneously maximizing and minimizing the dose delivered to tumors and OARs respectively, while producing sharp dose gradients at the transition between tumors and OARs. This problem has a conflicted objective because tumor(s) often intersect with OARs, and the dose deposition’s physics changes with each beam orientation so that BOO is a non-convex problem [1], [2] with myriad possible beam combinations within a robot’s phase space. Craft [1] locally tuned a beam angle set within the system’s continuous state space using linear programming duality theory, and found that the BOO problem for a simple 2D pancreatic case has about 100 minima when the optimization is warm-started from 100 different beam angles. Building on Craft’s work, Bertsimas et. al [3] resolved to a two meta-step algorithm: dynamically selecting beam angle candidates within the phase space via local minimum search with gradient descent, then exploring a different portion of the solution space by taking finite steps of simulated annealing. While [3] use global and local search with improvements in solutions obtained from equispaced angles, this method has the drawback of presenting the objective function as convex and assuming the doctor’s preferences can be represented as a set of linear constraints. Jia et. al [4] split the problem into two subproblems: first progressively identifying non-consequential beam angles by evaluating a multi objective function, and then optimizing the fluence on beam angles that are assigned a high confidence by a dosimetric objective function. Heuristic search strategies have also previously developed e.g. [5–7]. Other work treat IMRT treatment planning (TP) as an inverse optimization problem, with techniques ranging from adaptive l_{21} optimization [4], mixed integer linear programming [8–10] and simulated annealing [11, 12].

The BOO problem can be mathematically formulated as a set cover problem, where given a universe of all candidate beam angles, \mathcal{U} , we seek to find from a subset family \mathcal{S} of \mathcal{U} , a cover subfamily, $\mathcal{C} \subseteq \mathcal{S}$ whose union is an optimal beam set that meets a doctor’s prescription. This is a combinatorics problem where the parameters to be optimized increase to the extent that classical optimization methods become real-time infeasible. When just the robot’s tool frame is used to



Noninvasive RT. ©Novalis

adjust the fluence intensity, we have *coplanar beams*. In this work, we focus on finding good coplanar beams in BOO problems as commonly, only coplanar beams are employed [12]. We resort to an approximate dynamic programming (ADP) formulation to derive *approximately optimal policies* in high dimensional state spaces. Particularly, we leverage recent machine learning breakthroughs [13] to guide a Monte Carlo Tree Search

(MCTS) [14–16] of promising beam angle candidates by rapidly exploring different parts of the beam space. We reckon that having an automated toolset for choosing desirable beam angles will eradicate the manual search process, and save treatment time.

Contributions: We transform the BOO problem into a game planning strategy. Coupled with neural fictitious self-play, we refine the predictions from a neural network policy to drive the weights of the policy to a **saddle equilibrium** [17]. To this end,

- a deep neural network models the nonlinear dynamical system– generating policies that guide MCTS simulations for two players in a zero-sum Markov game
- the MCTS lookout strategy guides transition from one beam angle set to another during each markov decision process (MDP) setting for either player;
- each player finds a best response strategy to its opponent’s average strategy – driving the weights of the network policy toward an approximate **saddle equilibrium** [18].

2 Methods and Materials

Our design philosophy draws inspiration from approximate dynamic programming, optimal control theory, and game theory. For games with perfect information, there is an optimal value function, $v^*(s)$, that decides the game’s outcome for every possible state, $s \in \mathcal{S}$, under perfect play. One could therefore devise a planning strategy that guides the search for optimistic beam angle configurations within the setup’s phase space by using a probability distribution, $p(s, a)$, over a set of deterministic *pure strategies* for the tree.

The search for an *approximately* optimal beam angle set is performed by optimizing the parameters of a function approximator ψ , (here, a deep neural network, with multiple residual blocks as in [19]) that approximates a policy π , that guides MCTS simulations of ‘best-first’ beam angle combinations for a sufficiently large number of iterations. This MCTS performs a sparse lookout simulation, selectively adjusting beam angles that contribute the least to an optimal fluence. Successor nodes beneath a terminal node are **approximated** with a value, $v(s)$, to assure efficient selectivity. We maintain a probability distribution over possible states, based on a set of observation probabilities for the underlying MDP. Let us formalize definitions and notations used throughout the rest of this document.

2.1 Notations and Definitions

The state of the dynamical system is denoted by $s \in \mathcal{S}$; it is to be controlled by a discrete action $a \in \mathcal{A}$. States evolve according to the (unknown) dynamics $p(s_{t+1}|s_t, a_t)$, which we want to learn. The learning problem is posed within a discrete-time finite-time horizon, T , while a beam angle combination search task can be defined by a reward function, $r(s_t, a_t)$, which can be found by recovering a policy, $p(a_t|s_t; \psi)$, that specifies a distribution over actions conditioned on the state, and parameterized by the weights of a neural network, a tensor ψ . Without loss of generality, we denote the action conditional $p(a_t|s_t, \psi)$ as $\pi_\psi(a_t|s_t)$. Recovering the optimal weights may consist of the maximization problem

$$\psi^* = \arg \max_{\psi} \sum_{t=1}^T \mathbb{E}_{(s_t, a_t) \sim p(s_t, a_t | \psi)} [r(s_t, a_t)].$$

Definition 1. A **beam block** is a concatenation of beams, $\{\theta_1, \theta_2, \dots, \theta_m\}$ as a tensor of dimension $m \times C \times H \times W$ (see Fig. 1) that together with the patient’s ct mask form the state, s_t , at time step, t .

Definition 2. Every **node** of the tree, \mathbf{x} , has the following fields: (i) a pointer to the parent that led to it, $\mathbf{x}.p$; (ii) the beamlets, \mathbf{x}_b , stored at that node where $b = \{1, \dots, m\}$; (iii) a set of move probabilities prior, $p(s, a)$; (iv) a pointer, $\mathbf{x}.r$, to the reward, r_t , for the state s_t ; (v) a pointer to the state-action value $Q(s, a)$ and its upper confidence bound $U(s, a)$ (7) (vi) a visit count, $N(s, a)$, that indicates the number of times that node was visited; and (vii) a pointer $\mathbf{x}.child_i$ to each of its children nodes.

We want an adaptive allocation rule for determining the transition between states since we do not know what node may yield the best bandit, as a player might be biased

| Notation | Definition/Examples | Notation | Definition/Examples |
|------------------------------|--|-----------------------|---|
| m | dimensionality of a node’s beam set, e.g. $m = 5$ | n | dimension of discretized beam angles, e.g. $n = 180$ for 4° angular resolution |
| Θ | discretized beam angle set e.g. equally spaced angles between 0° and 360° , spaced apart at 4° | $a_t \in \mathcal{A}$ | control or action, $a_t \in \mathcal{A}$ at time step $t \in [1, T]$ used in determining the probability of transitioning from a beam angle subset to another within Θ |
| $\theta^j \subseteq \Theta$ | beam angles selected from Θ e.g. $\theta_k \in \mathbb{R}^m$ | $s_t \in \mathcal{S}$ | markovian system state at time step, $t \in [1, T]$ e.g. patient contour, beam angle candidates; dimensionality 2, 727, 936 to 3, 563, 520 |
| γ | discount factor e.g. 0.99 | \mathbf{f}_ψ | parametric function approximator (deep neural network policy) for state s_t |
| $v_\psi(s)$ | value estimate of state, s_t , as predicted by \mathbf{f}_ψ | $p(s)$ | probability distribution over current state, s generated by neural network policy |
| $Q(s, a)$ | action-state values that encode the “goodness” of a beam-angle set, $\theta_k \in \mathbb{R}^m$, where m is the number of beams considered for a fluence generation, e.g. $m = 5$ | \mathbf{B}_{x_t} | a concatenation of beams in consideration at time step, t , as a block of beams being fed to the neural network policy |
| $\mathcal{D}_{ij}(\theta_k)$ | dose matrix containing dose influence to voxel i from beam angle, θ_k , $\forall k \in \{1, 2, \dots, n\}$ where n is range of the beam set \mathcal{B} | \mathbf{D}_t | dose mask for target volume in consideration at time step, t |

Table 1: Table of notations commonly used in this article

towards always selecting the beams set with the maximum value. Therefore, we define the state broadly enough to capture all subjective unknowns that might influence the payoff/reward to be received by a rational decision-making agent; we then leverage the *upper confidence bound* algorithm of Agrawal [20] to assure an asymptotic logarithmic regret behavior. We attach a regret term $U(n(s))$ to the Q -value so as to ensure the optimal beam does not evade the simulation *i.e.* $Q(s, a) - U(n(s)) \leq Q(s, a) \leq Q(s, a) + U(n(s))$; the width of this confidence bound guides the exploration strategy for states that are momentarily unpromising in values but may later emerge as promising states. Other notations used in the article are delineated in Table 1.

2.2 Data Preprocessing

Patient Mask. We obtained 77 anonymized patient CT scans and their associated dose matrices. The scans relate to prostate cases used in previous IMRT treatment planning. The prostate data contains the scan of six organs, namely the patients’ body, bladder, left and right femoral heads, rectum, and planning target volume (PTV) or tumor. Each patient’s scan, D , is represented in 3D as $N \times W \times H$, where N is the total number of slices, W is the slice width and H is the slice height. We resized each slice to a square-shaped 2D matrix of size 64×64 . We generate 3D images that represent the orientation of the robot with respect to the patient for each discretized beam angle.

2.3 Neural Network Architecture

In addition to the resized masks, D , we define five feature planes, X_t as a block of beam configurations, B_{X_t} . B_{X_t} denotes the beam angles that generate the current fluence. For five beams for the fluence’s geometric shape for example, B_{X_t} would contain the 3D RGB images of the beams being considered at time step t . We augment the state with a memory of five previously used beam blocks, $\{B_{X_t}, \dots, B_{X_{t-5}}\}$.

The dose masks and beam blocks are as shown in Fig. 1. The input planes to the network are sized as $T \times N \times H \times W$ where T is the total number of input planes ($T = 6$ structures + 5 beams + 5×5 regressed beams = 36). Thus, the input to the network are arranged as: $s_t = [D_t, B_{X_t}, B_{X_{t-1}}, B_{X_{t-2}}, B_{X_{t-3}}, B_{X_{t-4}}, B_{X_{t-5}}]$. We use a modern neural network architecture with many residual blocks [19] so that each layer of the network fits a residual nonlinear mapping to its input data; we end up with a deeply stacked network whose input features, s_t , are processed by 34 residual blocks described as follows: (i) a 3D convolution with $64 \times l$ filters, a square kernel of width 7, and double strided convolutions, where l is the depth of the stack in the network; (ii) a 3D batch normalization layer [21]; (iii) nonlinear rectifiers [22]; (iv) a 3D convolution of $64 \times l$ filters; (v) a 3D batch normalization layer; (vi) a skip connection from the input to the block, in order to facilitate efficient gradients’ propagation; and (vii) nonlinear rectifiers.

We split the output of the network into two heads: (i) the first head is a probability distribution over which angle in the current beam block contributes the least to an optimal fluence cost at the current time step, while (ii) the second head estimates the *value* (in an *ADP sense*) of the subtree beneath the current node. This probability head is comprised of two residual blocks, each containing: (i) a 3D convolution of $64 \times l$ filters, followed by a square kernel of size 1, and a single strided convolution; (ii) a 3D batch normalization

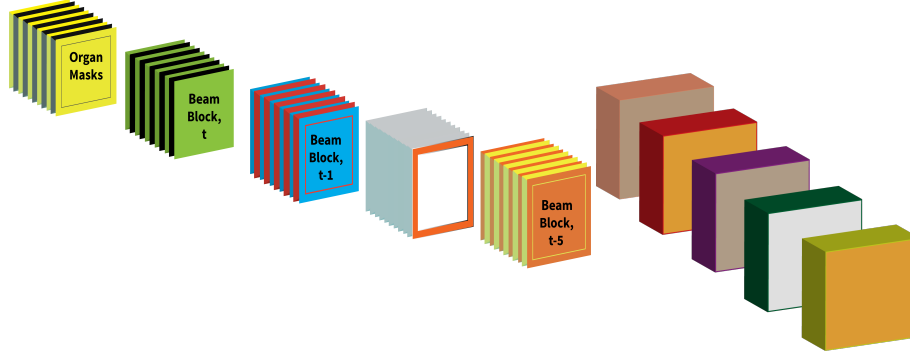


Fig. 1: [Left]: Concatenation of the target volume masks and the beam angles before feeding the input planes to the residual tower neural network. The first six planes (top-most mask of left figure) contain the delineated organs and the PTV. This is concatenated with a block of m beams from the current time step, regressed to the previous 5 time steps (here, 5 was heuristically chosen). [Right] Each beam angle in a beam block is represented as shown. Together with the target volume, these form an input plane of size $36 \times N \times W \times H$ to the policy/value neural network tower of residual blocks.

layer; (iii) nonlinear rectifiers; (iv) a 3D convolution of $64 \times l$ filters (v) a 3D batch normalization layer; (vi) a skip connection from the input to the block (vii) nonlinear rectifiers (viii) a fully connected layer that maps the resulting output to the total number of discretized beam angle grids; and (ix) a softmax layer then maps the neuron units to logit probabilities $p_i(s|a)$ for all beam angles.

The value head applies the following transformation modules (i) a 3D convolution of $64 \times l$ filters, a square kernel of size 1, and a single strided convolution; (ii) a 3D batch normalization layer; (iii) nonlinear rectifiers; (iv) a second 3D convolution of $64 \times l$ filters; (v) a 3D batch normalization layer; (vi) a skip connection from the input to the block (vii) nonlinear rectifiers and a sequential layer consisting of:

- a linear layer mapping the output of the above connections to a hidden 512-layer
- followed by a linear layer mapping to a 256 hidden unit, then rectified nonlinearities
- followed by a linear layer mapping to a scalar value, then rectified nonlinearities
- and a \tanh nonlinearity that maps the output to the closed interval $[-1, 1]$.

The network’s parameters were initialized using the proposal in [23]. The value and probability distribution heads are inspired from Bayesian decision theory, where it is expected that a rational decision-maker’s behavior is describable by a *utility function*, (or value function) – a quantitative characterization of the policy’s preferences for an outcome – and a subjective probability distribution, which describes the policy’s beliefs about all relevant unknown factors. When new information is presented to the decision-maker, the subjective probability distribution gets revised. Decisions about the optimal beam angle combination at the current time step are made under uncertainty; so we use a *probability model* to choose among **lotteries**, (*i.e.* probability distributions over all discretized beam angles in the setup). Each state during our learning process is constructed by appending the beam block at the current time step to a history of

beam blocks for the previous five time steps using a FIFO policy. Specifically, when we transition to a new state, the beam block that has been in the state set for the longest time (*i.e.* at the **head** of the queue) is deleted first, and the new state’s beam block is enqueued at the tail as in a **queue** data structure. This is so as to minimize the partial observability of the system.

2.4 Fluence Map Optimization

Suppose \mathcal{X} is the total number of discretized voxels of interest (*VOIs*) in a target volume, and $\mathcal{B}_1 \cup \mathcal{B}_2 \cup \dots \cup \mathcal{B}_n \subseteq \mathcal{B}$ represents the partition subset of a beam \mathcal{B} , where n is the total number of beams from which radiation can be delivered. Let $\mathcal{D}_{ij}(\theta_k)$ be the matrix that describes each dose influence, d_i , delivered to a discretized voxel, i , in a volume of interest, VOI_h ($h = 1, \dots, \mathcal{X}$), from a beam angle, θ_k , $k \in \{1, \dots, n\}$. One can compute the matrix $\mathcal{D}_{ij}(\theta_k)$ by calculating each d_i for every bixel, j , at every φ° , resolution, where $j \in \mathcal{B}_k$. Doing this, we end up with an ill-conditioned *sparse* matrix, $\mathcal{D}_{ij}(\theta_k)$, which consists of the dose to every voxel, i , incident from a beam angle, θ_k at every $360^\circ/\varphi^\circ$ (in our implementation, we set φ to 4°).

For a decision variable, x_j , representing the intensities of beamlets, it is trivial to find the dose influence, d_i , that relates the bixel intensities, x_j , to the voxels of interest, VOI_h . The fluence problem is to find the values of x_j for which d_i to the tumor is maximized, while simultaneously minimizing the d_i to critical structures. For the voxels in the target volume, a weighted quadratic objective minimizes the l_2 distance between a pre-calculated dose \mathbf{Ax} , and a doctor’s prescribed dose, \mathbf{b} , while a weighted quadratic objective maximizes the l_2 distance between \mathbf{Ax} (where \mathbf{x} represents the vectorized bixels, x_j) and \mathbf{b} . The pre-calculated dose term is given by $\mathbf{Ax} = \{\sum_s \frac{w_s}{v_s} \mathcal{D}_{ij}^s \mathbf{x}_s \mid \mathcal{D}_{ij} \in \mathbb{R}^{n \times l}, n > l\}$, which is a combination of the dose components that belong to OARs and those that belong to PTVs. Let $w_s = \{\underline{w}_s, \bar{w}_s\}$ represent the respective underdosing and overdosing weights for the OARs and PTVs, and v_s represents the total number of voxels in each structure. The cost function is

$$\frac{1}{v_s} \sum_{s \in \text{OARs}} \|(b_s - \underline{w}_s \mathcal{D}_{ij}^s \mathbf{x}_s)_+\|_2^2 + \frac{1}{v_s} \sum_{s \in \text{PTVs}} \|(\bar{w}_s \mathcal{D}_{ij}^s \mathbf{x}_s - b_s)_+\|_2^2 \quad (1)$$

where the underdosing weights are typically set as $\underline{w}_s = 0$ to deliver minimal dose to critical structures, while the overdosing weights are chosen to deliver the prescribed dose to the tumor; $(\cdot)_+$ denotes a Euclidean projection onto the nonnegative orthant \mathbb{R}_+ . We can succinctly write the above objective, subject to nonnegative bixel intensity constraints, as the minimization problem

$$\min \frac{1}{2} \|\mathbf{Ax} - \mathbf{b}\|_2^2 \quad \text{subject to } x \geq 0.$$

The Lagrangian becomes

$$L(\mathbf{x}, \boldsymbol{\lambda}) = \min \frac{1}{2} \|\mathbf{Ax} - \mathbf{b}\|_2^2 - \boldsymbol{\lambda}^T \mathbf{x}.$$

This problem can be solved with dual gradient descent (DGD), but DGD has the drawback that the primal and dual updates are not robust to objective’s constraints [24]. The

alternating direction method of multipliers (ADMM) [24] tackles the robustness problem by adding a quadratic penalty term to the Lagrangian and alternately updating the \mathbf{x} and $\boldsymbol{\lambda}$ variables in a “broadcast and gather” process. This turns out to be attractive since we will be solving a large-scale learning problem for the optimal beam angle set combination. Introducing an auxiliary variable \mathbf{z} , we have

$$\min_{\mathbf{x}} \frac{1}{2} \|\mathbf{A}\mathbf{x} - \mathbf{b}\|_2^2, \quad \text{subject to } \mathbf{z} = \mathbf{x}, \mathbf{z} \geq 0,$$

so that the Lagrangian can be written as,

$$\min_{\mathbf{x}, \mathbf{z}} \frac{1}{2} \|\mathbf{A}\mathbf{x} - \mathbf{b}\|_2^2 - \boldsymbol{\lambda}^T (\mathbf{z} - \mathbf{x}) + \frac{\rho}{2} \|\mathbf{z} - \mathbf{x}\|_2^2, \quad (2)$$

where $\boldsymbol{\lambda} \in \mathbb{R}^n$ is a multiplier and $\rho > 0$ is an ADMM penalty parameter. Minimizing (2) w.r.t \mathbf{x} , the \mathbf{x} subproblem of (2) yields

$$\min_{\mathbf{x}} \frac{1}{2} \mathbf{x}^T (\mathbf{A}^T \mathbf{A} + \rho \mathbf{I}) \mathbf{x} + (\boldsymbol{\lambda}^T - \mathbf{A}^T \mathbf{b} - \rho \mathbf{z}^T) \mathbf{x},$$

so that the \mathbf{x} -update (due to the convex quadratic nature of the problem) becomes,

$$\mathbf{x}^{k+1} = (\mathbf{A}^T \mathbf{A} + \rho \mathbf{I})^{-1} (\mathbf{A}^T \mathbf{b} + \rho \mathbf{z}^k - \boldsymbol{\lambda}^k). \quad (3)$$

Similarly, the \mathbf{z} -update for (2) can be found by the \mathbf{z} -minimization subproblem

$$\min_{\mathbf{z}} -\boldsymbol{\lambda}^T \mathbf{z} + \frac{\rho}{2} \|\mathbf{z} - \mathbf{x}\|_2^2 := \min_{\mathbf{z}} \frac{\rho}{2} \|\mathbf{z} - \mathbf{x} - \frac{1}{\rho} (\boldsymbol{\lambda})\|_2^2.$$

Using the soft-thresholding operator, $S_{\boldsymbol{\lambda}/\rho}$, we find that

$$\mathbf{z}^{k+1} = S_{\boldsymbol{\lambda}/\rho} (\mathbf{x}^{k+1} + \boldsymbol{\lambda}^k), \quad (4)$$

where $S_{\boldsymbol{\lambda}/\rho}(\tau) = (x - \boldsymbol{\lambda}/\rho)_+ - (-\tau - \boldsymbol{\lambda}/\rho)_+$. $\boldsymbol{\lambda}$ is updated as

$$\boldsymbol{\lambda}^{k+1} = \boldsymbol{\lambda}^k - \gamma (\mathbf{z}^{k+1} - \mathbf{x}^{k+1}), \quad (5)$$

where γ is a parameter that controls the step length. The inverse operation in (3) can be carried out with any iterative solver e.g. conjugate gradient. We use an over-relaxation parameter, $\alpha^k = 1.5$, and set the quadratic penalty to $\rho = 1.5$, in the \mathbf{z} and $\boldsymbol{\lambda}$ updates: $\alpha^k \mathbf{A} \mathbf{x}^{k+1} - (1 - \alpha^k) \mathbf{z}^k$. The stopping criterion is met when the primal and dual residuals are sufficiently small, *i.e.* ,

$$r^k = \|\mathbf{x}^k - \mathbf{z}^k\|_2 \leq \epsilon^{\text{pri}} \quad \text{and} \quad s^k = \|\rho (\mathbf{z}^{k+1} - \mathbf{z}^k)\|_2 \leq \epsilon^{\text{dual}},$$

with,

$$\epsilon^{\text{pri}} = \sqrt{\rho} \epsilon^{\text{abs}} + \epsilon^{\text{rel}} \max\{\|\mathbf{x}^k\|_2, \|\mathbf{z}^k\|_2\}, \quad \text{and}$$

$$\epsilon^{\text{dual}} = \sqrt{n} \epsilon^{\text{abs}} + \epsilon^{\text{rel}} (\rho \|\boldsymbol{\lambda}^k\|_2), \quad (6)$$

where $\epsilon^{\text{pri}} > 0$, $\epsilon^{\text{dual}} > 0$ are the primal and dual feasibility tolerances for the primal and dual feasibility conditions (see [24, §3.3]). We set $\epsilon^{\text{abs}} = 10^{-4}$ and $\epsilon^{\text{rel}} = 10^{-2}$.

2.5 Game Tree Simulation

Consider b^d possible move sequences of a robot-patient setup where b are the beam angles chosen to construct a fluence and d is the total number of discretized gantry angles. Suppose $b = 180$ and $d = 5$, we have 180^5 possible search directions, rendering exhaustive search infeasible. We leverage Monte Carlo simulations, encouraged by their recent success in large games [25–27], to break the curse of dimensionality [28].

We iteratively sample beam angles within the phase space by carrying out a lookahead search from the tree’s root node at a fixed depth, restricting samples to 90 discretized beams in Θ . At the first iteration, the subset of beam angles are randomly sampled from Θ . We then progressively add children nodes using an **expand_policy** (alg. 1), guided by *move probabilities* $p(s, a)$, generated by a network policy f_ψ , that either recursively **expands** the current node or rolls out the current simulation to completion.

As we recursively traverse the edges of the tree, we need to prevent “angle collisions”. We therefore introduce a minimum pairwise distance, $\bar{d}_i \in \mathbb{R}^+$ between the beamlets in a beam block, defined as $\|\theta_i - \theta_j\| \geq \bar{d}_i, \forall \{j \in m \setminus i\}$, with $\bar{d}_i = 20^\circ$. Repeatedly performing roll-outs, a history of state-action value pairs along the tree’s edges is kept; this ensures we can bias an action selection based on old actions that were chosen – aiding faster convergence if the same state is encountered more than once. We compute the mean outcome of every simulation through state s in which action a is selected, *i.e.* the tree’s $Q(s, a)$ -value, as $Q(s, a) = \frac{1}{N(s, a)} \sum_{i=1}^{n(s)} I_i(s, a) \zeta_i$, where $N(s, a) = \sum_{i=1}^{n(s)} I_i(s, a)$ is the total number of simulations in which action a was selected in state s , $n(s)$ is the total number of times a game is played through state s , and ζ_i is the outcome of the i th simulation played out from s . Specifically,

$$I_i(s, a) = \begin{cases} 1, & \text{if } a \text{ was selected on the } i\text{'th policy rollout} \\ 0, & \text{otherwise.} \end{cases}$$

During simulation, each state and action in the search tree are updated as: $n(s_t) \leftarrow n(s_t) + 1$; $N(s_t, a_t) \leftarrow N(s_t, a_t) + 1$; $Q(s_t, a_t) \leftarrow Q(s_t, a_t) + \pm r(s_t, a_t)$, where $r(s_t, a_t)$ is the reward/cost gained or incurred by the agent after action a in state s_t . After each simulation, a ‘best move’ for the current beam block is selected; we exponentiate the move probabilities by a temperature slightly larger than unity to encourage diversity in early play; specifically, we compute $p(a|s_0; \psi) = \frac{N(s_0, a)^{1/\tau}}{\sum_b N(s_0, b)^{1/\tau}}$, where τ is the temperature factor that diversifies the move probabilities. The modified UCT algorithm applied to optimal beam angle selection is presented in algorithm 1.

Definition 3. A minimizer player is at a **terminal state** if the FMO cost for the beams at a leaf node is greater than the cost of the beams at its direct ancestor node.

Definition 4. A maximizer player has reached a **terminal state** if the FMO cost for the beams at a leaf node is less than the FMO cost for the beams at its direct ancestor node.

Definition 5. We define an **upper confidence bound**, $U(s, a)$, on $Q(s, a)$ that adds an exploration bonus that is highest for seldomly visited state-action pairs so that the tree

Algorithm 1 Deep BOO Monte Carlo Tree Search

```

function MCTS( $s_0, c$ )
   $s_0 \leftarrow x_0(s_0)$ 
  while search_time < budget
  do
     $\bar{x} \leftarrow \text{EXPAND\_POLICY}(x_0, c)$ 
     $\bar{x}.r \leftarrow \text{FMO\_POLICY}(\bar{x})$ 
    BACKUP( $\bar{x}, \bar{x}.r$ )
  end while
  return BEST\_CHILD( $x_0$ )
end function

function SELECT\_MOVE( $x, c$ )
  if  $p_1$  to play then
    return  $\arg\max_{\bar{x} \in x} Q(\bar{x}) + \mathcal{K}(\bar{x})$ 
  else
    return  $\arg\min_{\bar{x} \in x} Q(\bar{x}) - \mathcal{K}(\bar{x})$ 
  end if
end function

function EXPAND\_POLICY( $x, c$ )
  while  $x$  nonterminal do
    if  $x$  not f.expanded then
      return EXPAND( $x, c$ )
    else
       $x \leftarrow \text{BEST\_CHILD}(x)$ 
    end if
  end while
  return  $x$ 
end function

function FMO\_POLICY( $x$ )
  return  $r = h^*(x(s)|\cdot)$ 
end function

function FULLY\_EXPANDED( $x, d$ )
   $d_i \leftarrow \text{pairwise\_distance}(x.s)$ 
  min_elem  $\leftarrow \min(d)$ 
  if min_elem <  $d$  then
    return True
  else
    return False
  end if
end function

function EXPAND( $x, c$ )
   $\bar{a} = \text{SELECT\_MOVE}(x, c)$ 
  sample  $\bar{\theta}$  with  $x.p(s, a)$ 
  update  $\bar{\theta} \leftarrow \bar{\theta} + \bar{a}$ 
  with  $\pi_{t-1}$ , create  $\bar{x}.p(\bar{s}, \bar{a})$ 
  while not  $\bar{x} \in x_0$  do
    add  $\bar{x}$  to  $x$ 
  end while
  return  $\bar{x}$ 
end function

function BACK\_UP( $x, \bar{x}.r$ )
  while  $\bar{x}$  not null do
     $N(\bar{x}) \leftarrow \bar{x} + 1$ 
     $Q(\bar{x}) \leftarrow Q(\bar{x}) + \bar{x}.r$ 
     $\bar{x} = \text{parent of } \bar{x}$ 
  end while
end function

function BEST\_CHILD( $x_0$ )
  if  $p_1$  to play then
    return  $x_0[\arg\min \text{ children of } x_0.r]$ 
  else
    return  $x_0[\arg\max \text{ children of } x_0.r]$ 
  end if
end function

```

where $\mathcal{K}(\bar{x}) = c\sqrt{\frac{2 \ln n(\bar{x}.s)}{N(\bar{x}.s, a)}}$ and $\bar{x} \in x$ implies $\bar{x} \in \text{children of } x$.

expansion policy selects the action a^* that maximizes the augmented value:

$$\bar{Q}(s, a) = Q_j(s, a) + c\sqrt{\frac{2 \ln n(s)}{N(s, a)}}, \quad \text{where } a^* = \arg \max_a \bar{Q}(s, a). \quad (7)$$

$Q(s, a)$ is the highest average observed reward from node j – encouraging exploitation of the current node, and $\ln n(s)$ is the natural logarithm of the total number of roll-outs through state s . The second term in (7) encourages exploration of other beam angles and c is a scalar exploration constant.

Note that (7) is a version of the **UCB1** algorithm [16] and definitions 3 and 4 preserve the neighborhood search for the beam tuning as specified earlier. We continually update the weights of the neural network policy in a separate thread, writing the weights to a shared memory buffer for the MCTS to read from, *i.e.* the search thread uses the previous iteration of the trained network policy to to run the policy improvement procedure. When angles are at the edges *i.e.* 0° or 360° and an angle change outside the range $0 \leq \theta \leq 360$ is recommended, we “wrap” around to enforce cyclicity. Note that the **EXPAND_POLICY** and **FMO_POLICY** procedures of alg. 1 can be seen as a form of Add/Drop simulated annealing as described in [12]. While the **FMO_POLICY** procedure returns the node with the optimal fluence cost, the **BEST_CHILD** procedure compares the quality of all beam angle sets in the children of the tree’s root node.

2.6 Self-Play Neuro-Dynamic Programming

We consider an approximate dynamic programming (ADP) setting whose task is to discover the mapping between patient’s geometry and a set of good beam angle combinations by maximizing an extrinsic reward signal that is stage-wise informed by the quality of a fluence profile. The goal here is to find an ideal set of neural network weights that narrows the focus for the search for desirable beam angles to a desirable portion of the beam space. To this end, we apply optimal control of incompletely known **MDPs** [29]. The MDP consists of states $s \in \mathcal{S}$, actions, $a \in \mathcal{A}$, transition probability, $\mathcal{P}_{ss'}^a$, and a reward function \mathcal{R}_s^a . $\mathcal{P}_{ss'}^a$ governs states evolution from $s \rightarrow s'$, while \mathcal{R}_s^a determines stage-wise rewards after transitions.

To find a good saddle-point for the optimization problem, we applied weakened fictitious self-play (FSP) [18] to find an *approximate* best response strategy to an opposing agent’s mixed strategy in Markov decision games. In our formulation, each player does not necessarily know the strategy of its opponent ahead of time *i.e.* their security levels do not necessarily coincide. To ensure that equilibrium can be found within *pure strategies*, we let one player act after observing the decision outcome of the other player.

The network, \mathbf{f}_ψ , predicts a probability distribution over all beam angle configurations, $p_a = p(s, a)$, and a *value*, $v_\psi(s)$ – an estimate that the current beam angle set θ may be the optimal beam set. For a game, Γ , suppose that $y = \{y_1, \dots, y_m \mid \sum_{i=1}^m y_i = 1\}$ and $z = \{z_1, \dots, z_n \mid \sum_{i=1}^n z_i = 1\}$ are the respective probability distributions for players p_1 and p_2 , defined on the n and m –dimensional simplices respectively, the average value of the game will correspond to player p_1 minimizing a cost $\mathcal{J}(y, z) = y^T \Gamma z$ and player p_2 maximizing $\mathcal{J}(y, z)$. Each player’s action is governed by a mixed strategy – obtained by adding a Gaussian random walk sequence with standard deviation 2 to the prior probability distribution predicted by the neural network policy or computed by the tree policy; this is then normalized by the sum of the resulting noised distribution. Players p_1 , and p_2 ’s strategies are independent random variables, repeatedly implemented during game simulations. As the number of times the game is played gets larger, the

frequency with which different actions for p_1 and p_2 are chosen will converge to the probability distribution that characterize their random strategies [30, pp.24].

Each MDP episodic setting involves randomly sampling from the CT dataset, concatenating the sampled geometry to the previous beam blocks, and eliminating the beam that has been longest in the block as in a *FIFO* scheme. States are modified based on the probability predicted by policy, $\pi(\cdot)$, which along with the patient’s state, s_t , (including the current and previous five beam block configuration) result in a new node. Between node transitions, a full FMO is carried out – evaluating the quality of chosen beamlets, and informing updates in search probabilities that we later compute when we reach a terminal leaf.

The network policy, $\pi(\cdot|\psi_t)$, and search tree, $\Gamma(\pi_\psi(\cdot))$, are optimized in separate concurrent threads; to assure non-blocking of search and network optimization processes, the network’s weights were written to a shared memory map, where they are asynchronously updated by gradient descent, while the tree search thread ran in a parallel thread from a previous iteration of the network policy, $\pi(\cdot|\psi_{t-1})$. At the end of a full MDP iteration, we compare the value predicted by either player, average their mixing strategies and update the gradients of the loss function with respect to the *values* based on equation (8). We train the probability distribution over current beams by maximizing the similarity between the computed search probabilities π and the predicted distribution \mathbf{p} (by the search process) with the cross-entropy loss:

$$\Delta\psi_p = \frac{\log \partial \mathbf{p}_\psi(a|s)}{\partial \psi} (\pi^T \mathbf{p}),$$

and we take the network weights’ induced tensor norm (last term of (8) given its robustness to the assymetrical network modular weights). Altogether, we minimize the combined loss,

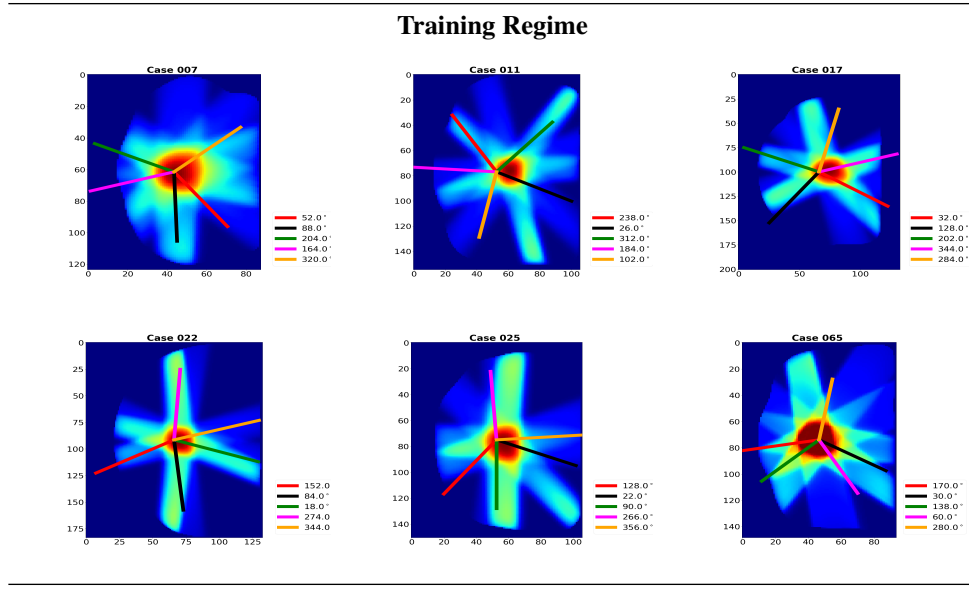
$$l = (\zeta - v)^2 - \pi^T \mathbf{log}(\mathbf{p}) + \lambda \|\psi\|_2^2, \quad (8)$$

where λ (set to 1.5) controls regularization of the network weights to avoid overfitting. The cross entropy term was weighted by 0.9, and the mean square error (mse) loss by 0.01 to keep the overall loss in the direction of persistent reduction in training error. These values were found by empirical evaluations of the loss surface. We use 4 search threads, 8 CPUs, and 4 GPUs for the final version of this algorithm.

3 Results

This section presents results on 3D prostate cases. We start the training process by randomly adding five beam blocks at first to the state queue as described in §2. The input planes are then passed through the tower residual network, from which probability distributions and a value are predicted. We add a random walk sequence to the generated pure strategy from the neural network and construct our tree with this mixed strategy (at subsequent iterations, a previous iteration of the neural network is used to generate the mixed strategy used to run the tree search). As new beam angle combinations are found according to Algorithm 1, the FIFO queue is updated. When the tree search terminates, we compute new search probabilities and perform the backward pass of the algorithm.

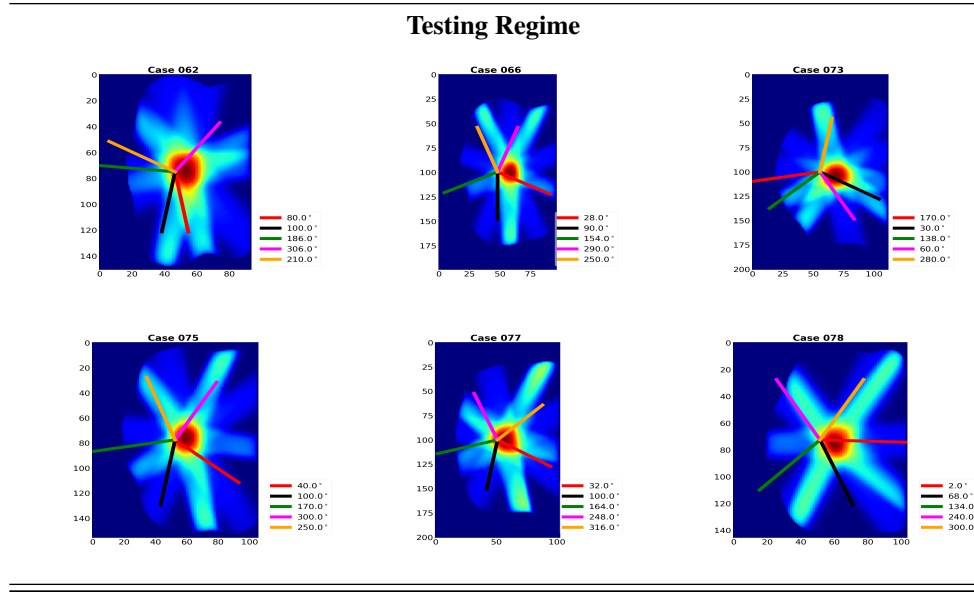
Table 2: Dose wash plots for select patients during training of the self-play network



The mixed strategy is a by-product of the prediction by the deep neural network policy; it guides search for optimistic beam angles, based on a reward (or cost) that is maximized (or minimized) by either of players p_1 or p_2 . When a move is selected (see alg. 1), the current node is expanded, resulting in a new set of beamlets. The fluence (using eq. (1)) for the beamlets are optimized and the reward for maximizing player, or the cost of the minimizing player are updated. We continue the expansion of the leaves until we reach a terminal leaf.

The displayed plots in Table 2 are the dose washes we obtain by optimizing the fluence (a resultant of the beam angles chosen) on the patient. The wash plots are effects achieved by the display of the voxel intensities (in 2D) according to the organs, and tumors present in a target volume slice. They enable us to interpret the quality of a dose based on the organs that must be targeted (*i.e.* tumors) and organs that must be avoided (*i.e.* critical structures). The dosage is represented as a heat map. Regions that receive zero radiation are dark blue, while regions that receive higher doses progress in the order of higher intensity from green through yellow to red. As seen, the intersection of beams delivers heavy doses to the tumors while largely sparing moderate surrounding tissues. The line overlays on the plots depict the angle of incident radiation. The effectiveness of our results best understood by visualizing the central slices in each target volume since it often contains the most organs in a 3D volume. Table 3 describes the inference results. The policy selects fairly equidistant beams, yielding wash plots that provide good dosimetric concentration on the tumor (center of the slices shown) and sharp gradients at the transition between tumors and OARs, while also largely avoiding strong dose to OARs. The advantage of this policy is that finding the right beam angles is orders of magnitude faster than the current way these angles are found in the clinic. At test time,

Table 3: Dose wash plots for select patients during testing of self-play network



we pick the last checkpoint during training and use it to find feasible beam angles. The search process typically takes between 2-3 minutes before we settle on a good candidate beam angle set. This is significant time saved compared to manually tuning beam angles by dosimetrists or radiation therapists in clinics.

4 Conclusions

Beam orientation optimization is a key component of treatment planning optimization with a nonconvex solution surface given the way the dose coefficients can significantly alter based on the angle from which beams are aimed to a target volume. As such, in modern clinics, solving this problem involves many hours of planning, tuning and refinement – usually by experienced treatment planners. Given the long time traditional optimization approaches take in solving this problem, we adopt a hybrid approach, leveraging Monte Carlo simulation of games in high dimensional state-spaces, neurodynamic programming, convex optimization of fluence profiles, and game theory to arrive at good candidate beamlets. Our work is the first, to the best of our knowledge, that transforms the BOO problem into a MCTS strategy with pseudocode. Successive work will incorporate DVH constraints into the search strategy in order to obtain more robust beam angles, and investigate using more than five beam angles to test the limits of fluence optimality for patients.

References

1. Craft, D.: Local beam angle optimization with linear programming and gradient search. *Physics in Medicine & Biology* **52**(7), N127 (2007) [2](#)
2. Södertröm, S., Brahme, A.: Optimization of the Dose Delivery In A Few Field Techniques Using Radiobiological Objective Functions. *Medical physics* **20**(4), 1201–1210 (1993) [2](#)
3. Bertsimas, D., Cacchiani, V., Craft, D., Nohadani, O.: A Hybrid Approach To Beam Angle Optimization In Intensity-modulated Radiation Therapy. *Computers & Operations Research* **40**(9), 2187–2197 (2013) [2](#)
4. Jia, X., Men, C., Lou, Y., Jiang, S.B.: Beam Orientation Optimization For Intensity Modulated Radiation Therapy Using Adaptive L2,1-minimization. *Physics in Medicine and Biology* **56**(19), 6205–6222 (2011) [2](#)
5. Bortfeld, T., Schlegel, W.: Optimization of beam orientations in radiation therapy: Some theoretical considerations. *Physics in Medicine & Biology* **38**(2), 291 (1993) [2](#)
6. Djajaputra, D., Wu, Q., Wu, Y., Mohan, R.: Algorithm and Performance Of A Clinical Imrt Beam-angle Optimization System. *Physics in Medicine & Biology* **48**(19), 3191 (2003) [2](#)
7. Pugachev, A., Xing, L.: Computer-assisted selection of coplanar beam orientations in intensity-modulated radiation therapy. *Physics in Medicine & Biology* **46**(9), 2467 (2001) [2](#)
8. Wang, C., Dai, J., Hu, Y.: Optimization of beam orientations and beam weights for conformal radiotherapy using mixed integer programming. *Physics in Medicine & Biology* **48**(24), 4065 (2003) [2](#)
9. Lim, G.J., Ferris, M.C., Wright, S.J., Shepard, D.M., Earl, M.A.: An optimization framework for conformal radiation treatment planning. *INFORMS Journal on Computing* **19**(3), 366–380 (2007) [2](#)
10. D D'Souza, W., Meyer, R.R., Shi, L.: Selection of beam orientations in intensity-modulated radiation therapy using single-beam indices and integer programming. *Physics in Medicine & Biology* **49**(15), 3465 (2004) [2](#)
11. Hou, Q., Wang, J., Chen, Y., Galvin, J.M.: Beam orientation optimization for imrt by a hybrid method of the genetic algorithm and the simulated dynamics. *Medical Physics* **30**(9), 2360–2367 (2003) [2](#)
12. Aleman, D.M., Kumar, A., Ahuja, R.K., Romeijn, H.E., Dempsey, J.F.: Neighborhood Search Approaches to Beam Orientation Optimization in Intensity Modulated Radiation Therapy Treatment Planning. *Journal of Global Optimization* **42**(4), 587–607 (2008) [2](#), [11](#)
13. LeCun, Y., Bengio, Y., Hinton, G.: Deep Learning. *Nature* **521**(7553), 436–444 (2015) [2](#)
14. Gelly, S., Silver, D.: Monte-Carlo tree search and rapid action value estimation in computer Go. *Artificial Intelligence* **175**, 1856–1875 (2011) [3](#)
15. Coulom, R.: Efficient Selectivity and Backup Operators in Monte-Carlo Tree Search. *International Conference on Computers and Games* (2006) [3](#)
16. Kocsis, L., Szepesvári, C.: Bandit based Monte-Carlo Planning. *European Conference on Machine Learning* (2006) [3](#), [11](#)
17. Ogunmolu, O., Gans, N., Summers, T.: Minimax Iterative Dynamic Game : Application to Nonlinear Robot Control. *IEEE International Conference on Intelligent Robots and Systems* (2018) [3](#)
18. Heinrich, J., Lanctot, M., Silver, D.: Fictitious self-play in extensive-form games. In: *International Conference on Machine Learning*, pp. 805–813 (2015) [3](#), [11](#)
19. He, K., Zhang, X., Ren, S., Sun, J.: Deep Residual Learning For Image Recognition. In: *Proceedings of the IEEE conference on computer vision and pattern recognition*, pp. 770–778 (2016) [3](#), [5](#)
20. Agrawal, R.: Sample mean based index policies by o (log n) regret for the multi-armed bandit problem. *Advances in Applied Probability* **27**(4), 1054–1078 (1995) [5](#)

21. Ioffe, S., Szegedy, C.: Batch Normalization: Accelerating Deep Network Training By Reducing Internal Covariate Shift. arXiv preprint arXiv:1502.03167 (2015) [5](#)
22. Hahnloser, R.H., Sarpeshkar, R., Mahowald, M.A., Douglas, R.J., Seung, H.S.: Digital selection and analogue amplification coexist in a cortex-inspired silicon circuit. *Nature* **405**(6789), 947 (2000) [5](#)
23. He, K., Zhang, X., Ren, S., Sun, J.: Delving Deep into Rectifiers: Surpassing Human-level Performance on Imagenet Classification. In: Proceedings of the IEEE international conference on computer vision, pp. 1026–1034 (2015) [6](#)
24. Boyd, S., Parikh, N., Chu, E., Peleato, B., Eckstein, J.: Distributed Optimization and Statistical Learning via the Alternating Direction Method of Multipliers. *Foundations and Trends in Machine learning* **3**(1), 1–122 (2011) [7](#), [8](#)
25. Chung, M., Buro, M., Schaeffer, J.: Monte carlo planning in rts games. In: CIG. Citeseer (2005) [9](#)
26. Silver, D., Huang, A., Maddison, C.J., Guez, A., Sifre, L., Van Den Driessche, G., Schrittwieser, J., Antonoglou, I., Panneershelvam, V., Lanctot, M., Dieleman, S., Grewe, D., Nham, J., Kalchbrenner, N., Sutskever, I., Lillicrap, T., Leach, M., Kavukcuoglu, K., Graepel, T., Hassabis, D.: Mastering the game of Go with deep neural networks and tree search. *nature* 529, no. 7587: 484–489. (2016) [9](#)
27. Silver, D., Schrittwieser, J., Simonyan, K., Antonoglou, I., Huang, A., Guez, A., Hubert, T., Baker, L., Lai, M., Bolton, A., et al.: Mastering the Game Of Go Without Human Knowledge. *Nature* **550**(7676), 354 (2017) [9](#)
28. Bellman, R.: Dynamic programming. Princeton University Press (1957) [9](#)
29. Astrom, K.: Optimal Control of Markov Processes with Incomplete State Information **10**, 174–205 (1965) [11](#)
30. Basar, T., Olsder, G.J.: Dynamic noncooperative game theory, vol. 23. Siam (1999) [12](#)